Dose distribution of the brain tissue associated with cognitive functions in high-grade glioma patients

J Jacob, E Clausse, M A Benadjaoud, C Jenny, M Ribeiro, L Feuvret, J-J Mazeron, D Antoni, M-O Bernier, K Hoang-Xuan, et al.

Dose distribution of the brain tissue associated with cognitive functions in high-grade glioma patients

Distribution de dose aux tissus cérébraux impliqués dans les fonctions cognitives chez les patients porteurs d'un gliome de haut grade

Julian Jacob[a, b]; Emmanuelle Clausse[c]; Mohamed Amine Benadjaoud[d]; Catherine Jenny[c]; Monica Ribeiro[b, e]; Loïc Feuvret[a]; Jean-Jacques Mazeron[a] ; Delphine Antoni[f]; Marie-Odile Bernier[g]; Khê Hoang-Xuan[e, h]; Dimitri Psimaras[e, h]; Alexandre Carpentier[h, i]; Damien Ricard[b, j, k]; Philippe Maingon[a].

[a] Sorbonne University, Assistance Publique-Hôpitaux de Paris, GH Pitié-Salpêtrière-Charles Foix, Department of Radiation Oncology, Paris, France.

[b] University Sorbonne Paris Cité, CNRS, Service de Santé des Armées, COGNAC-G - Cognition and Action Group, Paris, France.

[c] Sorbonne University, Assistance Publique-Hôpitaux de Paris, GH Pitié-Salpêtrière-Charles Foix, Department of Medical Physics, Paris, France.

[d] Radiobiology and Regenerative Medicine Research Service, Direction of Human Health, Institut de Radioprotection et de Sûreté Nucléaire, Fontenay-aux-Roses, France.

[e] Sorbonne University, Assistance Publique-Hôpitaux de Paris, GH Pitié-Salpêtrière-Charles Foix, Department of Neurology 2-Mazarin, Paris, France.

[f] University of Strasbourg, Centre Paul Strauss, University Radiotherapy Department, Strasbourg, France.

[g] Laboratory of Epidemiology, Institut de Radioprotection et de Sûreté Nucléaire, Fontenay-aux-Roses, France.

[h] Sorbonne University, INSERM, CNRS, Assistance Publique-Hôpitaux de Paris, Institut du Cerveau et de la Moelle épinière, Paris, France.

[i] Sorbonne University, Assistance Publique-Hôpitaux de Paris, GH Pitié-Salpêtrière-Charles Foix, Department of Neurosurgery, Paris, France.

[j] Service de Santé des Armées, Hôpital d'Instruction des Armées Percy, Department of Neurology, Clamart, France.

[k] Service de Santé des Armées, Ecole du Val-de-Grâce, Paris, France.

Auteur correspondant: Dr. Julian Jacob - GH Pitié-Salpêtrière-Charles Foix - Department of Radiation Oncology - 47-83, boulevard de l'Hôpital – 75013 Paris, France - Téléphone: 00 33 1 84 82 74 90 – Fax: 00 33 1 42 17 81 30 - E-mail: julian.jacob@aphp.fr

Ce travail a été présenté au Congrès Annuel de l'Association des Neuro-Oncologues d'Expression Française (ANOCEF) le 14 juin 2019 à Poitiers et récompensé du prix de la meilleure communication orale de la session « Traitements focaux ».

Remerciements: adressés au Dr. Mostefa Bourkaib et à ses collaborateurs pour la correction de la traduction en anglais, à Mme. Françoise Culot, Mme. Elisabeth Le Corre ainsi qu'à M. Haysam Salman pour leur aide technique.

Titre courant: Doses to the areas implied in cognition

RESUME

Objectif: L'objectif de cette étude prospective dosimétrique était d'évaluer la distribution de dose en regard des aires cérébrales impliquées dans les fonctions cognitives selon deux techniques: arcthérapie volumétrique modulée (VMAT) et tomothérapie hélicoïdale (HT).

Patients et méthodes: Trente-sept patients ont été traités pour un glioblastome sus-tentoriel selon une technique VMAT à base de deux arcs entre 2016 et 2018. Une dose totale de 60 Gy en 30 fractions quotidiennes a été administrée au volume cible prévisionnel (PTV). Les structures cérébrales occupant une place importante dans la physiologie cognitive, comme les hippocampes, le corps calleux, le cervelet, les zones péri-ventriculaires (ZPV), ont été délinées. Pour chaque patient, un nouveau plan de traitement en HT a été déterminé en aveugle par une seconde physicienne médicale selon les mêmes contraintes de dose et priorités. Les analyses statistiques ont été menées à l'aide du test des rangs signés de Wilcoxon.

Résultats: Les indices de conformité étaient similaires entre les deux techniques. Les valeurs moyennes étaient de 0,96 (0,19-1,00) en VMAT et de 0,98 (0,84-1,00) en HT, respectivement (p=0,73). Des réductions significatives de la $D_{50\%}$ ont été observées en VMAT comparativement à la HT: 14,6 Gy (3,8-28,0) contre 17.4 Gy (12,1-25,0) pour l'encéphale sain (p=0,014); 32,5 Gy (10,3-60,0) contre 35,6 Gy (17,1-58,0) pour le corps calleux (p=0,038); 8,1 Gy (0,4-34,0) contre 12,8 Gy (0,8-27,0) pour le cervelet (p<0,001), respectivement.

Conclusion: La technique VMAT semblait améliorer la protection des principales régions cérébrales impliquées dans les fonctions cognitives sans compromettre la couverture du PTV.

Mots clés: gliome; fonctions cognitives; radiothérapie conformationnelle par modulation d'intensité.

SUMMARY

Purpose: The purpose of this prospective dosimetric study was to assess the dose distribution regarding brain areas implied in cognitive functions using two approaches: volumetric modulated arc therapy (VMAT) and helical tomotherapy (HT).

Patients and methods: Thirty-seven patients were treated using a dual-arc VMAT approach for supratentorial glioblastoma between 2016 and 2018. The total dose of 60 Gy in 30 daily fractions was administered to the planning target volume (PTV). Brain structures that play an important role in cognitive physiology, such as the hippocampi, corpus callosum, cerebellum, subventricular zones (SVZ), were delineated. For each patient, a new treatment plan in HT was determined by a second medical physicist in a blindly fashion according to the same dose constraints and priorities. Statistical analyses were performed using the Wilcoxon-signed rank test.

Results: Conformity indexes remained similar with both techniques. The mean values were 0.96 (0.19-1.00) for VMAT and 0.98 (range, 0.84-1.00) for HT, respectively (p=0.73). Significant $D_{50\%}$ reductions were observed with VMAT compared to HT: 14.6 Gy (3.8-28.0) versus 17.4 Gy (12.1-25.0) for the normal brain (p=0.014); 32.5 Gy (10.3-60.0) versus 35.6 Gy (17.1-58.0) for the corpus callosum (p=0.038); 8.1 Gy (0.4-34.0) versus 12.8 Gy (0.8-27.0) for the cerebellum (p<0.001), respectively.

Conclusion: The VMAT approach seemed to improve the sparing of the key brain areas implied in cognitive functions without jeopardizing PTV coverage.

Keywords: glioma; cognitive functions; intensity modulated radiation therapy.

INTRODUCTION

In patients with high-grade glioma (HGG), radiotherapy represents one of the major treatments options; however, it is associated with adverse events like cognitive impairment, which can alter various functions, occur during the first 4 months following brain irradiation and persist more than one year after the last radiotherapy session [1]. Complex multimodal mechanisms are implicated in the brain injuries induced by radiotherapy with inflammation and oxidative stress leading to the occurrence of neurologic disturbances [2]. Cognitive impairment following brain radiotherapy could be related to dosimetric factors, like the delivered total dose and dose per fraction [3]. The knowledge of the cerebral areas' radiosensitivity has to be improved.

The hippocampi are cerebral structures that play a highly important role in cognition and their dysfunction could lead to memory impairment according to preclinical data [4]. Statistically significant correlations between the doses delivered to the hippocampi and late decline in neuropsychological tests performed following focal brain radiotherapy have been highlighted [5]. Following these results, radiation techniques sparing the hippocampi, especially using intensity-modulated radiation therapy (IMRT) approaches have been developed [6].

Cognitive impairment following brain radiotherapy can also be explained by the exposure of areas such as the white matter, subventricular zones (SVZ) or cerebral cortex [7-9]. Indeed, in patients treated with focal brain radiotherapy, early modifications of parahippocampal cingulum observed in Diffusion Tensor Imaging (DTI) seemed to predict the late decline reported in the Hopkins Verbal Learning Test [7]. IMRT sparing the SVZ, a niche of adult neurogenesis, has shown promising results by reducing the cognitive adverse events in patients with HGG [8]. A dose effect relationship was reported regarding the

cerebral cortical thickness measured using magnetic resonance imaging (MRI) one year after the end of focal brain radiotherapy [9].

An ongoing prospective study has been following patients treated with chemoradiotherapy for HGG, namely by performing neuropsychological assessments, recording the doses delivered to the healthy brain tissues and assessing the morphological changes using MRI [10].

The reported dosimetric work, focused on IMRT approaches, has for purpose to compare the dose distributions to cerebral areas implied in cognition in patients treated with RapidArc volumetric modulated arc therapy (VMAT) to the plans performed in helical tomotherapy (HT) using the data prospectively collected in the context of the aforementioned study.

PATIENTS AND METHODS

Patient selection

This prospective study was approved by the institutional review boards of the recruiting centres. The inclusion and exclusion criteria have been previously reported [10]. All included patients provided written informed consent. Histological diagnosis of HGG, i.e. World Health Organization (WHO) grade III or IV glioma, was established following surgical resection or biopsy. Chemoradiotherapy indication was decided in a multidisciplinary setting. Concurrent chemotherapy with temozolomide 75 mg/m^2/day was administered seven days a week from the first until the last radiotherapy session.

All recruited patients were treated with focal brain radiotherapy. Among 138 patients enrolled in this study since 2015, 80 were treated with three-dimensional conformal

radiotherapy and not considered for analyses. IMRT was administered to 56 patients using VMAT, HT or static IMRT for 38, 12 and 6 patients, respectively. The IMRT technique attribution was not randomized nor related to the PTV location but based on the equipment availabilities. The treatment plan of one patient treated with hypofractionated radiotherapy due to older age was not taken into account. Missing data were noted for one patient.

Finally, thirty-seven consecutive patients treated with normofractionated VMAT for supratentorial grade IV glioma between 2016 and 2018 were considered (**Table 1**). Thirty-four (91.9%) and three (8.1%) patients were right- and left-handed, respectively.

Radiotherapy techniques

For each patient, computed tomography (CT) images were acquired with a slice thickness of 2.5 mm from the vertex to the hyoid bone using a General Electric© LightSpeed 16 system. Patients were immobilised in a supine position using a thermoplastic head contention device. No iodine infusion was given. All patients underwent brain MRI during the two weeks before the radiotherapy start according to the following protocol: axial projection, squared matrix, T1-weighted sequences with and without gadolinium-enhanced, T2 fluid attenuated inversion recovery. Delineation of the target volumes and organs at risk (OAR) was performed using the Eclipse™ software (version 13.5, Varian© Medical Systems, Palo Alto, California) with merging of CT-scan and MRI images. Gross and clinical target volume definition was performed following the European Society for Radiotherapy and Oncology guidelines [11]. Isotropic tridimensional margins of 3 mm were applied to the clinical target volume to generate the planning target volume (PTV). OAR usually studied in daily practice were delineated, namely the brainstem and optic pathways [12]. Specific brain areas playing a highly important role in cognition were defined: cerebellum, corpus callosum, frontal lobes,

hippocampi, SVZ, temporal lobes [13, 14]. Twin structures' dosimetric data were individually registered and reported according to the location related to the PTV (ipsilateral or contralateral brain hemisphere). Other healthy tissues were delineated: the posterior cerebral fossa, corresponding to the addition of the brainstem to the cerebellum, the normal supratentorial region and the normal brain, i.e. the supratentorial area and the whole brain from which was extracted the PTV, respectively. All cerebral areas were defined on the MRI T1-weighted sequences and checked on the CT-scan (**Figure 1**).

Treatment planning

For each patient, the prescribed dose to the PTV was 60 Gy delivered in 30 daily fractions using 6-MV X-ray beams in a single-phase plan. The dosimetric study was performed using the Eclipse™ treatment planning system (TPS) version 13.5. The VMAT approach (RapidArc) was planned using two full or partial coplanar arcs. The dedicated linear accelerator was the Varian TrueBeam® STx, using High Definition 120-leaf multileaf collimator 2.5-mm width (centre), 5 mm-width (peripheral). Dose prescription and target volume coverage followed the guidelines of the International Commission on Radiation Units and Measurements Report 83 [15]. Dose constraints to the healthy organs had to respect previously published recommendations [16]. The dose to 40% of both hippocampi should have not exceeded 7.3 Gy [5]. High priority OAR were: the brainstem, the optic pathways and the normal brain.

All the acquired data were then transferred to the Artiview™ (Aquilab®, Loos, France) version 3.24.3 dedicated platform. The PTV coverage was assessed using the following parameters: the homogeneity index (HI), the conformity index (CI) and the Paddick index (PI), defined by the respective formulas:

- HI = $(D_{2\%}-D_{98\%})/D_{50\%}$ [15];
- CI = V_{PI}/V_{PTV} [15];
- PI = $(V_{PTV} \cap V_{PI})^2 / (V_{PTV} \text{ x } V_{PI})$ [17],

where $D_{98\%}$, $D_{50\%}$ and $D_{2\%}$ corresponded to the calculated doses to 98%, 50% and 2% of the PTV, respectively. V_{PTV} and V_{PI} respectively referred to the PTV extent and to the volume of the prescription isodose, i.e. 95% or 57 Gy.

The differences of calculated doses related to each technique were assessed for each dose level considering the structure volume. The results were reported using dose-volume histograms with the y-axis expressing the dose difference between VMAT and HT and the x-axis referring to the percentage of the exposed structure.

Also, the estimated total treatment time was also calculated using monitor units (MU), the maximum dose rates of 400 MU and 895 MU per minute being considered in the treatment planning for the VMAT and HT approaches, respectively.

Statistical analyses

Comparison between techniques for the dosimetric parameters, i.e. the median dose ($D_{50\%}$), PTV coverage and number of MU, was performed using the Wilcoxon-signed rank test. The dosimetric distribution comparison was assessed using a pointwise comparison between the Dx considered as functions defined on the interval [0,1] (range of the x percentages). Within this framework, the 95% confidence intervals (CI) were generated using the bootstrap approach [18]. The testing procedure proposed by Smaga et al. was used to infer the difference between paired sample mean functions [19]. The level of significance was defined as $p<0.05$ according to the Benjamini–Hochberg discovery rate correction [20]. All

analyses were performed using the MATLAB® software (version 8.2.0.701, R2013b, MathWorks©, Natick, Massachusetts).

RESULTS

Planning target volume coverage

Mean CI values were 0.96 (range, 0.19-1.00) and 0.98 (range, 0.84-1.00) with VMAT and HT, respectively (p=0.73). A significant difference between VMAT and HT was observed for mean PI values: 0.82 (range, 0.19-0.94) and 0.74 (range, 0.55-0.86), respectively (p<0.001).

The mean PTV $D_{98\%}$ were 57.1 Gy (range, 41.2-58.9) with VMAT and 57.3 Gy (range, 44.0-59.8) with HT, respectively (p=0.31). The mean PTV $D_{50\%}$ were 60.0 Gy (range, 56.2-60.5) with VMAT and 59.7 Gy (range, 59.1-60.0) with HT, respectively (p<0.001). The mean PTV $D_{2\%}$ were 61.6 Gy (range, 57.9-62.3) with VMAT and 60.6 Gy (range, 60.2-61.4) with HT, respectively (p<0.001). The mean HI were calculated at 0.07 (range, 0.04-0.34) with VMAT and 0.05 (range, 0.01-0.30) with HT, respectively (p<0.001).

Healthy cerebral tissue exposure

The mean $D_{50\%}$ to the brain areas that are associated with cognitive functions are reported in **Table 2**. The respective decreases in the doses to 10%, 33% and 66% of the normal brain were of 6.3 Gy, 3.3 Gy and 2.9 Gy with VMAT versus HT (p<0.001; **Figure 2A**). The normal supratentorial area exposure was also significantly reduced with VMAT (p<0.001; **Figure 2B**).

The cerebellum and the posterior cerebral fossa were also significantly less exposed with VMAT ($p<0.001$ in both analyses; **Figures 3A and 3B**).

A borderline significant trend towards an improved sparing of the hippocampus ipsilateral to the PTV was observed for the doses delivered to 90% of this structure, with a reduction exceeding 2 Gy using VMAT compared with HT ($p=0.12$; **Figure 4A**). No statistically significant difference was observed regarding the dose delivered to 40% of the ipsilateral hippocampus. The contralateral hippocampus exposure was similar considering both techniques ($p=0.11$; **Figure 4B**).

The dose to the corpus callosum was reduced with VMAT compared with HT, notably regarding the highest dose levels ($p=0.011$; **Figure 5**).

The ipsilateral and contralateral frontal lobes were significantly less exposed with VMAT than with HT, especially at low dose levels ($p=0.001$ and $p=0.003$, respectively; **Figures 6A and 6B**). Significant dose reductions were also reported for the ipsilateral and contralateral temporal lobes with VMAT ($p=0.006$ and $p=0.002$, respectively; **Figures 7A and 7B**).

The ipsilateral subventricular zone was less exposed with VMAT, especially at high dose levels ($p=0.018$; **Figure 8A**). A similar trend was observed in the contralateral subventricular zone ($p=0.068$; **Figure 8B**).

Treatment time

The mean time required to deliver one single fraction was significantly reduced with VMAT: 502 MU (range, 353-821), i.e. 1.3 minutes (range, 0.9-2.1), versus 2625 MU (range, 2006-3372), i.e. 2.9 minutes (range, 2.2-3.8), with HT, respectively ($p<0.001$).

DISCUSSION

This dosimetric study in 37 patients treated with normofractionated IMRT for glioblastoma highlighted a significant dose reduction to the OAR associated with cognitive functions using VMAT compared with HT. PTV coverage was not significantly jeopardized, despite the HI improvement observed with HT. Treatment time was also significantly shorter with VMAT. These results confirmed the previously published data suggesting the dosimetric improvements related to IMRT, especially to VMAT, in glioblastoma patients [21].

The HT features used in this study were specific to the centre where the patients were referred to. The differences in terms of jaw thickness (2.5 cm in the presented work), could modify the dosimetric results [22]. The healthy tissue sparing could be improved using thinner jaws at the expense of the time per fraction.

VMAT using the dual-arc technique seemed to protect efficiently the healthy tissues. Briere et al. reported a trend to an improved sparing of the ipsilateral hippocampus with VMAT planned using two or three arcs versus step-and-shoot IMRT, with a reduction of the dose delivered to 100% of this area (19.7 Gy versus 31.7 Gy; p=0.03, not statistically significant) [23]. Similar observations were reported for the mean and maximal doses. The mean and maximal doses to the contralateral hippocampus tended to be higher with VMAT. No difference was observed in terms of normal brain exposure. The use of full or partial arcs, based namely on PTV location and extent, could also modify the OAR exposure [24].

Two limitations of this work were the small cohort size and the interobserver variability. Intraobserver modifications had to be avoided by working with two experimented medical physicists performing individually treatment plans using two different IMRT approaches, VMAT and HT. Although dose limitations and priorities remained the same, the interobserver variability has to be considered, especially regarding the OAR for which no

dose constraint has been defined yet. Other parameters could be different between series, namely the PTV extent and location. No relevant statistical analysis could be performed to assess the PTV location effect on the dose distribution to the OAR due to the small cohort size.

In the presented work, statistically significant dose reductions to several brain areas implied in cognitive functions have been reported with VMAT compared with HT plans. These results could suggest a clinical benefit of the VMAT approach by an improved healthy tissue sparing. This trend has to be confirmed in a higher number of patients. The consequences of these dosimetric differences on the cognitive functions remain highly unknown and require further investigation using neuropsychological assessments. In a prospective study led on 23 patients treated for primary brain tumours, Huynh-Le et al. reported the minimum dose to the corpus callosum and the volume of right-sided subcortical white matter exposed to total doses of 30 or 40 Gy could predict the attention/processing speed decrease observed 6 months after radiotherapy [25]. Another prospective study performed on 20 low-grade glioma patients treated with protontherapy showed no significant cognitive decline with a median follow-up of 36 months regarding the neuropsychological assessments [26]. Tabrizi et al. reported no statistically significant relationship between the risk of cognitive impairment following brain radiotherapy and the dose distribution to the healthy tissues, namely to the hippocampi.

While hippocampal-sparing radiotherapy techniques have been widely studied, the protection of other brain areas could also have clinical implications. Morphological modifications of the white matter beneath the anterior cingulate cortex highlighted with DTI predicted significant decline in executive functions in patients treated with either photons or with protons for primary brain tumours [27]. Cerebral cortex sparing using namely IMRT has also been developed in a series of 10 glioblastoma patients [28]. A retrospective study in 52

patients showed a dose-dependent reduction in amygdala volume one year after the completion of focal brain radiotherapy [29]. Hence, the protection of these nuclei located close to the hippocampi could be clinically relevant. Identification of the cortical brain areas highly sensitive to radiotherapy could help to develop new techniques in order to improve patients' quality of life [30].

CONCLUSION

This prospective dosimetric study performed in 37 patients with glioblastoma demonstrated significantly improved healthy tissue sparing with VMAT compared with HT without jeopardizing PTV coverage. The next objectives of this work are namely to prospectively assess the cognitive decline related to the exposure of the healthy brain areas using neuropsychological tests and to evaluate the morphological changes using MRI one year after the last radiotherapy session. Consequently, an individual dosimetric mapping could help to propose relevant dose constraints to the cerebral areas implied in cognition.

Conflict of interest: none.

REFERENCES

[1] Makale MT, McDonald CR, Hattangadi-Gluth JA, Kesari S. Mechanisms of radiotherapy-associated cognitive disability in patients with brain tumours. Nat Rev Neurol 2017;13:52-64.

[2] Jacob J, Durand T, Feuvret L, Mazeron JJ, Delattre JY, Hoang-Xuan K, et al. Cognitive impairment and morphological changes after radiation therapy in brain tumors: A review. Radiother Oncol 2018;128:221-8.

[3] Soussain C, Ricard D, Fike JR, Mazeron JJ, Psimaras D, Delattre JY. CNS complications of radiotherapy and chemotherapy. Lancet 2009;374:1639-51.

[4] Tomé WA, Göhkan Ş, Gulinello ME, Brodin NP, Heard J, Mehler MF, et al. Hippocampal-dependent neurocognitive impairment following cranial irradiation observed in pre-clinical models: current knowledge and possible future directions. Br J Radiol 2016;89:20150762.

[5] Gondi V, Hermann BP, Mehta MP, Tomé WA. Hippocampal dosimetry predicts neurocognitive function impairment after fractionated stereotactic radiotherapy for benign or low-grade adult brain tumors. Int J Radiat Oncol Biol Phys 2013;85:348-54.

[6] Hofmaier J, Kantz S, Söhn M, Dohm OS, Bächle S, Alber M, et al. Hippocampal sparing radiotherapy for glioblastoma patients: a planning study using volumetric modulated arc therapy. Radiat Oncol 2016;11:118.

[7] Chapman CH, Nagesh V, Sundgren PC, Buchtel H, Chenevert TL, Junck L, et al. Diffusion tensor imaging of normal-appearing white matter as biomarker for radiation-induced late delayed cognitive decline. Int J Radiat Oncol Biol Phys 2012;82:2033-40.

[8] Redmond KJ, Ye X, Assadi RK, McIntyre R, Moore J, Ford EC, et al. Neural progenitor cell (NPC) sparing radiation therapy (RT) plus temozolomide (TMZ) in newly diagnosed glioblastoma multiforme (GBM) associated with neurocognitive function but not tumor outcomes: results of a prospective clinical trial. [Abstract] Int J Radiat Oncol Biol Phys 2015;93 Suppl:S111.

[9] Karunamuni R, Bartsch H, White NS, Moiseenko V, Carmona R, Marshall DC, et al. Dose-Dependent Cortical Thinning After Partial Brain Irradiation in High-Grade Glioma. Int J Radiat Oncol Biol Phys 2016;94:297-304.

[10] Durand T, Jacob S, Lebouil L, Douzane H, Lestaevel P, Rahimian A, et al. EpiBrainRad: an epidemiologic study of the neurotoxicity induced by radiotherapy in high grade glioma patients. BMC Neurol 2015;15:261.

[11] Niyazi M, Brada M, Chalmers AJ, Combs SE, Erridge SC, Fiorentino A, et al. ESTRO-ACROP guideline “target delineation of glioblastomas”. Radiother Oncol 2016;118:35-42.

[12] Scoccianti S, Detti B, Gadda D, Greto D, Furfaro I, Meacci F, et al. Organs at risk in the brain and their dose-constraints in adults and in children: a radiation oncologist’s guide for delineation in everyday practice. Radiother Oncol 2015;114:230-8.

[13] Barani IJ, Cuttino LW, Benedict SH, Todor D, Bump EA, Wu Y, et al. Neural stem cell-preserving external-beam radiotherapy of central nervous system malignancies. Int J Radiat Oncol Biol Phys 2007;68:978-85.

[14] Eekers DB, In ‘t Ven L, Roelofs E, Postma A, Alapetite C, Burnet NG, et al. The EPTN consensus-based atlas for CT- and MR-based contouring in neuro-oncology. Radiother Oncol 2018;128:37-43.

[15] International Commission on Radiation Units and Measurements. ICRU Report 83: Prescribing, Recording, and Reporting Photon-Beam Intensity-Modulated Radiation Therapy (IMRT). J ICRU 2010;10;1-106.

[16] Noël G, Antoni D, Barillot I, Chauvet B. [Delineation of organs at risk and dose constraints]. Cancer Radiother 2016;20 Suppl:S36-60.

[17] Paddick I, Lippitz B. A simple dose gradient measurement tool to complement the conformity index. J Neurosurg 2006;105 Suppl:194-201.

[18] Efron B, Tibshirani RJ. An introduction to the Bootstrap. 1st ed. New York: Chapman & Hall/CRC Monographs on Statistics and Applied Probability; 1994.

[19] Smaga Ł. A note on repeated measures analysis for functional data. AStA Advances in Statistical Analysis 2019;https://doi.org/10.1007/s10182-018-00348-8.

[20] Benjamini Y, Hochberg Y. Controlling the False Discovery Rate: A Practical and Powerful Approach to Multiple Testing. J R Stat Soc Series B Stat Methodol 1995;57:289-300.

[21] Amelio D, Lorentini S, Schwarz M, Amichetti M. Intensity-modulated radiation therapy in newly diagnosed glioblastoma: a systematic review on clinical and technical issues. Radiother Oncol 2010;97:361-9.

[22] Saw CB, Katz L, Gillette C, Koutcher L. 3D treatment planning on helical tomotherapy delivery system. Med Dosim 2018;43:159-67.

[23] Briere TM, McAleer MF, Levy LB, Yang JN. Sparing of normal tissues with volumetric arc radiation therapy for glioblastoma: single institution clinical experience. Radiat Oncol 2017;12:79.

[24] Bas Ayata H, Ceylan C, Kılıç A, Güden M, Engin K. Comparison of Multiple Treatment Planning Techniques for High-Grade Glioma Tumors Near to Critical Organs. Oncol Res Treat 2018;41:514-9.

[25] Huynh-Le MP, Tringale KR, Karunamuni R, Marshall DC, Burkeen J, Seibert TM, et al. Dosimetric Predictors of Cognitive Decline in Attention and Processing Speed after Fractionated Brain Radiation Therapy. Int J Radiat Oncol Biol Phys 2018;102 (3 Suppl):S171.

[26] Tabrizi S, Yeap BY, Sherman JC, Nachtigall LB, Colvin MK, Dworkin M, et al. Long-term outcomes and late adverse effects of a prospective study on proton radiotherapy for patients with low-grade glioma. Radiother Oncol 2019;137:95-101.

[27] Tringale KR, Nguyen T, Bahrami N, Marshall DC, Leyden KM, Karunamuni R, et al. Identifying early diffusion imaging biomarkers of regional white matter injury as indicators of executive function decline following brain radiotherapy: A prospective clinical trial in primary brain tumor patients. Radiother Oncol 2019;132:27-33.

[28] Exeli AK, Kellner D, Exeli L, Steininger P, Wolf F, Sedlmayer F, et al. Cerebral cortex dose sparing for glioblastoma patients: IMRT versus robust treatment planning. Radiat Oncol 2018;13:20.

[29] Huynh-Le MP, Karunamuni R, Moiseenko V, Farid N, McDonald CR, Hattangadi-Gluth JA, et al. Dose-dependent atrophy of the amygdala after radiotherapy. Radiother Oncol 2019;136:44-9.

[30] Nagtegaal SHJ, David S, van der Boog ATJ, Leemans A, Verhoeff JJC. Changes in cortical thickness and volume after cranial radiation treatment: A systematic review. Radiother Oncol 2019;135:33-42.

LEGENDES DES TABLEAUX ET FIGURES

Tableau 1: Caractéristiques des patients (n= 37).

Tableau 2: Doses médianes aux tissus cérébraux sains selon la technique de radiothérapie.

Figure 1: Coupe axiale d'imagerie par résonance magnétique en séquence T1 associée à la tomodensitométrie dosimétrique: délinéation des volumes cibles macroscopique, anatomo-clinique et prévisionnel (en rouge, bleu et orange, respectivement) et des régions cérébrales impliquées dans les fonctions cognitives: corps calleux (en violet), zones péri-ventriculaires gauche et droite (en marron et cyan, respectivement), lobes frontaux gauche et droit (en blanc et jaune, respectivement).

Figure 2: Comparaisons des distributions de doses au niveau de l'encéphale sain (Figure 2A) et de la région sus-tentorielle saine (Figure 2B).

Figure 3: Comparaisons des distributions de doses en regard du cervelet (Figure 3A) et de la fosse cérébrale postérieure (Figure 3B).

Figure 4: Comparaisons des distributions de doses à l'hippocampe ipsilatéral (Figure 4A) et à l'hippocampe controlatéral (Figure 4B).

Figure 5: Comparaison des distributions de doses au corps calleux.

Figure 6: Comparaisons des distributions de doses au lobe frontal ipsilatéral (Figure 6A) et au lobe frontal controlatéral (Figure 6B).

Figure 7: Comparaisons des distributions de doses au lobe temporal ipsilatéral (Figure 7A) et au lobe temporal controlatéral (Figure 7B).

Figure 8: Comparaisons des distributions de doses à la zone péri-ventriculaire ipsilatérale (Figure 8A) et à la zone péri-ventriculaire controlatérale (Figure 8B).

TRANSLATIONS OF TABLE AND FIGURE LEGENDS

Table 1: Patient characteristics (n= 37).

Table 2: Median doses to the healthy brain areas according to the radiotherapy technique.

Figure 1: Magnetic resonance imaging T1-weighted sequence axial slice merged with the dosimetric computed tomography-scan: delineation of the gross, clinical, planning target volumes (in red, blue and orange, respectively) and of the brain areas implied in cognitive functions: corpus callosum (in purple), left and right subventricular zones (in brown and cyan, respectively), left and right frontal lobes (in white and yellow, respectively).

Figure 2: Comparisons of dose distributions to the normal brain (Figure 2A) and to the normal supratentorial area (Figure 2B).

Figure 3: Comparisons of dose distributions to the cerebellum (Figure 3A) and the posterior cerebral fossa (Figure 3B).

Figure 4: Comparisons of dose distributions to the ipsilateral hippocampus (Figure 4A) and to the contralateral hippocampus (Figure 4B).

Figure 5: Comparison of dose distributions to the corpus callosum.

Figure 6: Comparisons of dose distributions to the ipsilateral frontal lobe (Figure 6A) and to the contralateral frontal lobe (Figure 6B).

Figure 7: Comparisons of dose distributions to the ipsilateral temporal lobe (Figure 7A) and to the contralateral temporal lobe (Figure 7B).

Figure 8: Comparisons of dose distributions to the ipsilateral subventricular zone (Figure 8A) and to the contralateral subventricular zone (Figure 8B).

Table 1

Feature	n (% or range)
Gender	
Male	28 (75.7%)
Female	9 (24.3%)
Median age in years (range)	59 (29-72)
Median Karnofsky Performance Status before radiotherapy in percentages (range)	90 (70-100)
Median planning target volume in cm^3 (range)	214 (72-550)
Planning target volume location	
Left frontal lobe	2 (5.4%)
Right frontal lobe	9 (24.3%)
Left temporal lobe	11 (29.8%)
Right temporal lobe	6 (16.2%)
Left parietal lobe	6 (16.2%)
Right parietal lobe	1 (2.7%)
Left occipital lobe	1 (2.7%)
Right occipital lobe	1 (2.7%)
Extent of surgery	
Gross total resection	22 (59.5%)
Subtotal resection	8 (21.6%)
Biopsy	7 (18.9%)

Table 2

Organ at risk	Median dose in Gy (range)				p-value
	VMAT		HT		
Cerebellum	8.1	(0.4-34.0)	12.8	(0.8-27.0)	<0.001
Corpus callosum	32.5	(10.3-60.0)	35.6	(17.1-58.0)	0.038
Frontal lobe					
Ipsilateral	28.0	(1.9-60.0)	32.4	(7.0-60.0)	0.001
Contralateral	16.1	(1.3-41.0)	18.3	(5.0-52.0)	0.027
Hippocampus					
Ipsilateral	39.1	(1.4-60.0)	39.4	(2.5-60.0)	0.813
Contralateral	12.8	(1.2-44.0)	11.8	(1.9-55.0)	0.469
Normal brain	14.6	(3.8-28.0)	17.4	(12.1-25.0)	0.014
Posterior cerebral fossa	9.4	(0.4-36.0)	13.8	(0.9-27.0)	<0.001
SVZ					
Ipsilateral	40.0	(9.1-60.0)	44.8	(19.9-60.0)	0.004
Contralateral	20.9	(3.1-43.0)	22.6	(6.5-47.0)	0.149
Supratentorial area – PTV	16.6	(6.8-28.0)	17.6	(13.1-26.0)	0.339
Temporal lobe					
Ipsilateral	38.0	(1.1-61.0)	40.9	(2.0-60.0)	0.002
Contralateral	12.4	(0.9-26.0)	12.8	(1.5-39.0)	0.637

Abbreviations: HT: Helical Tomotherapy, PTV: Planning Target Volume, SVZ: Subventricular zone, VMAT: Volumetric Modulated Arc Therapy.

Figure 1

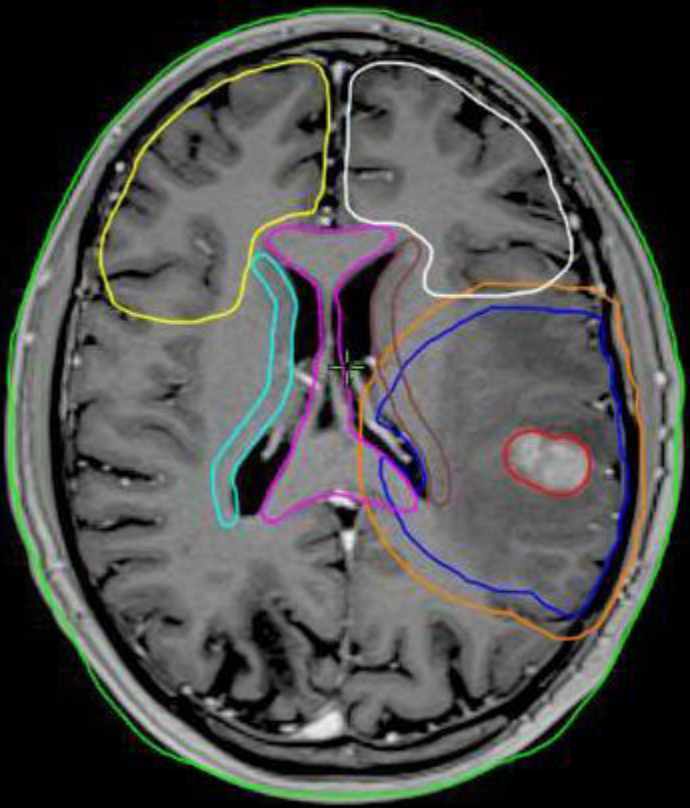

Figure 2A

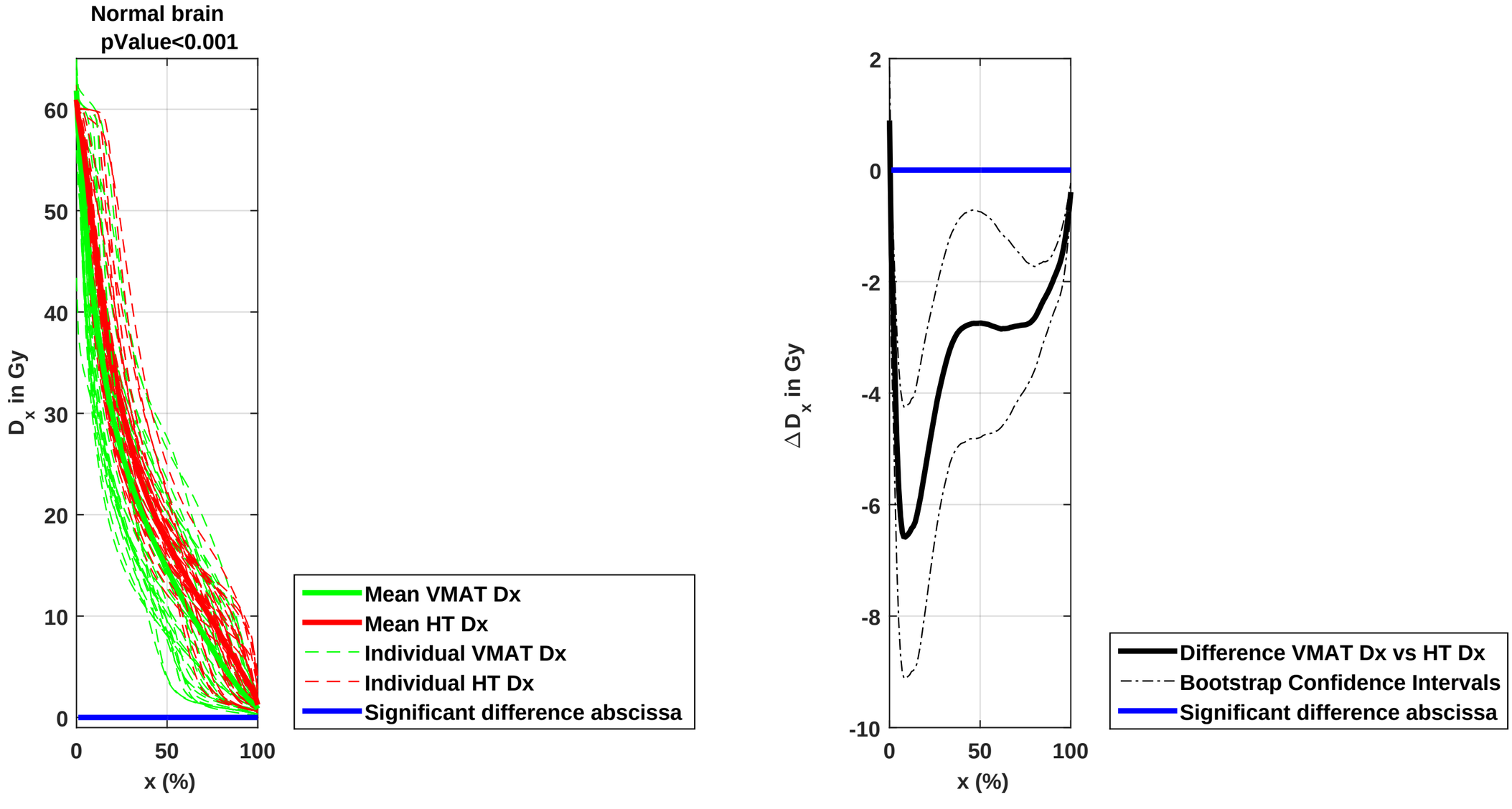
Normal brain
pValue<0.001
D_x in Gy
x (%)
Mean VMAT Dx
Mean HT Dx
Individual VMAT Dx
Individual HT Dx
Significant difference abscissa
△D_x in Gy
x (%)
Difference VMAT Dx vs HT Dx
Bootstrap Confidence Intervals
Significant difference abscissa

Figure 2B

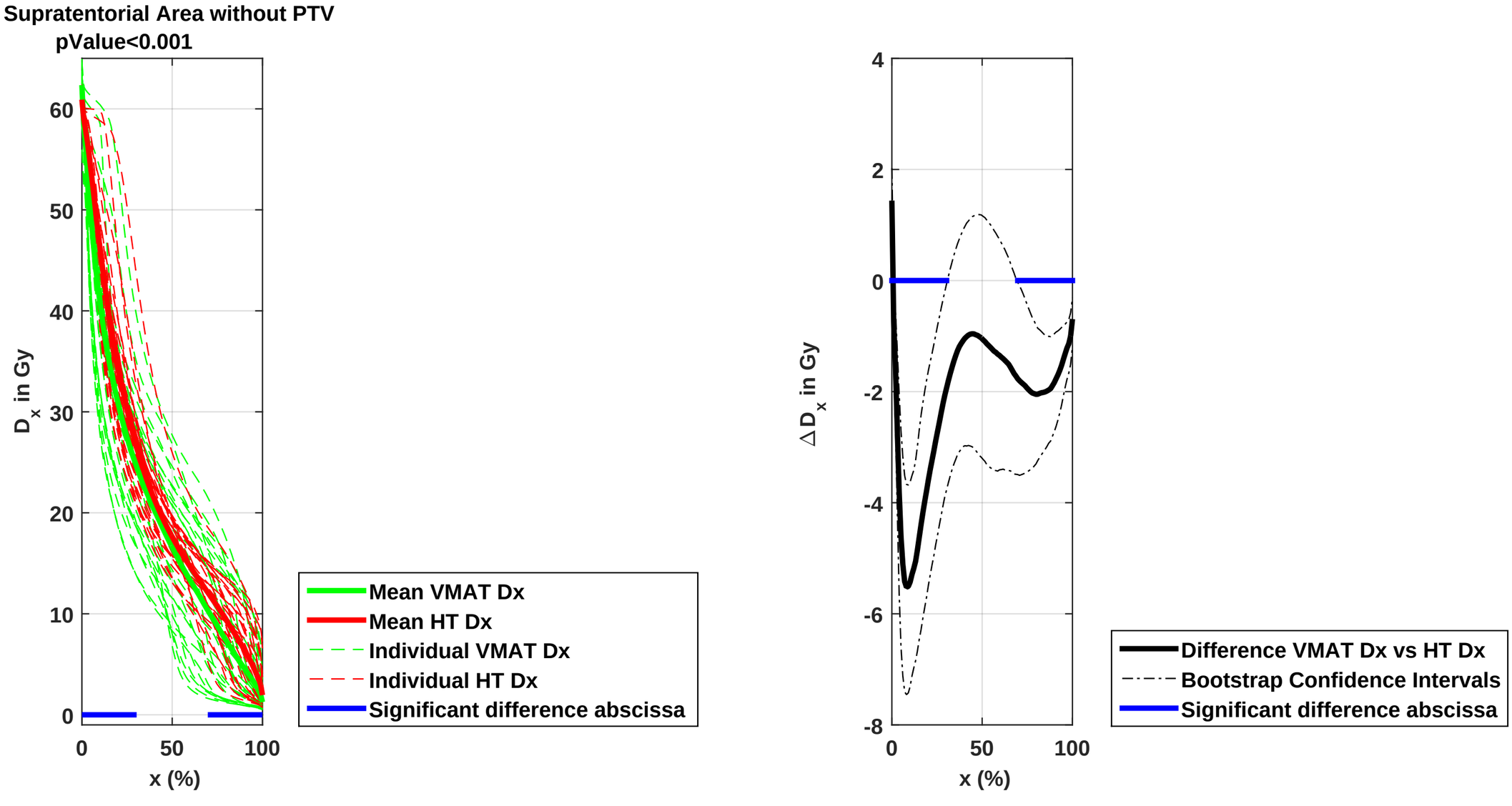
Supratentorial Area without PTV
pValue<0.001
D_x in Gy
x (%)
Mean VMAT Dx
Mean HT Dx
Individual VMAT Dx
Individual HT Dx
Significant difference abscissa
ΔD_x in Gy
x (%)
Difference VMAT Dx vs HT Dx
Bootstrap Confidence Intervals
Significant difference abscissa

Figure 3A

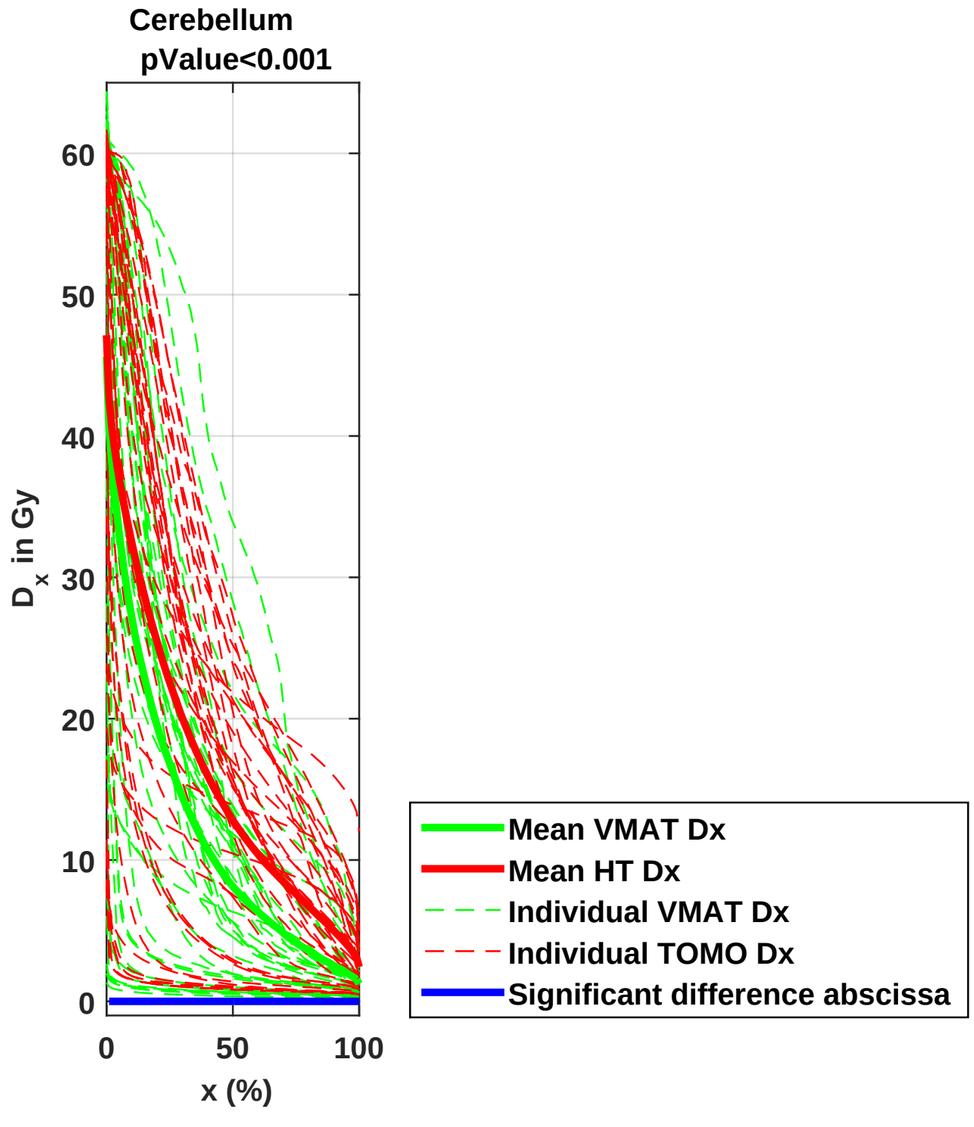
Cerebellum
pValue<0.001
D_x in Gy
x (%)
0
10
20
30
40
50
60
0
50
100
Mean VMAT Dx
Mean HT Dx
Individual VMAT Dx
Individual TOMO Dx
Significant difference abscissa

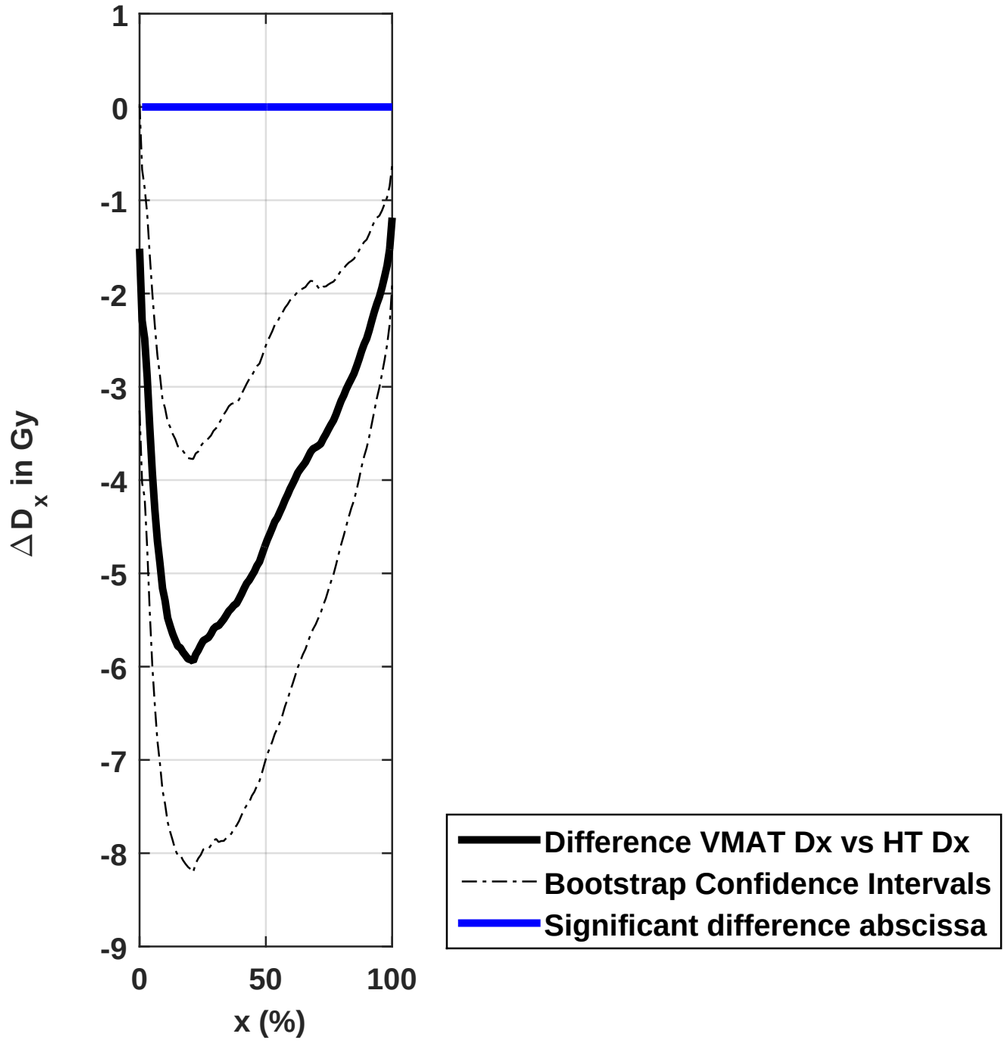
ΔD_x in Gy
x (%)
1
0
-1
-2
-3
-4
-5
-6
-7
-8
-9
0
50
100
Difference VMAT Dx vs HT Dx
Bootstrap Confidence Intervals
Significant difference abscissa

Figure 3B

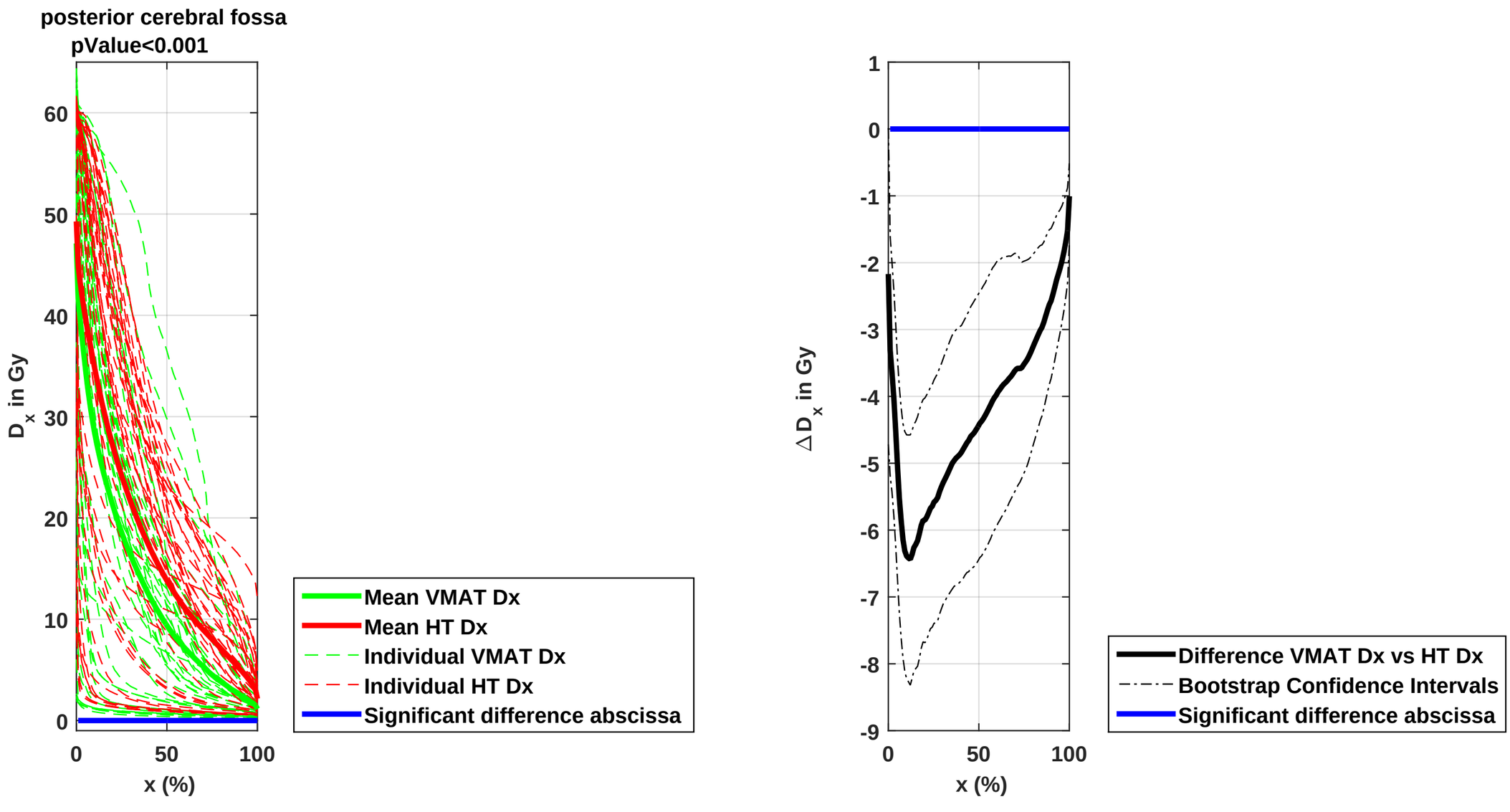
posterior cerebral fossa
pValue<0.001
D_x in Gy
x (%)
Mean VMAT Dx
Mean HT Dx
Individual VMAT Dx
Individual HT Dx
Significant difference abscissa
ΔD_x in Gy
x (%)
Difference VMAT Dx vs HT Dx
Bootstrap Confidence Intervals
Significant difference abscissa

Figure 4A

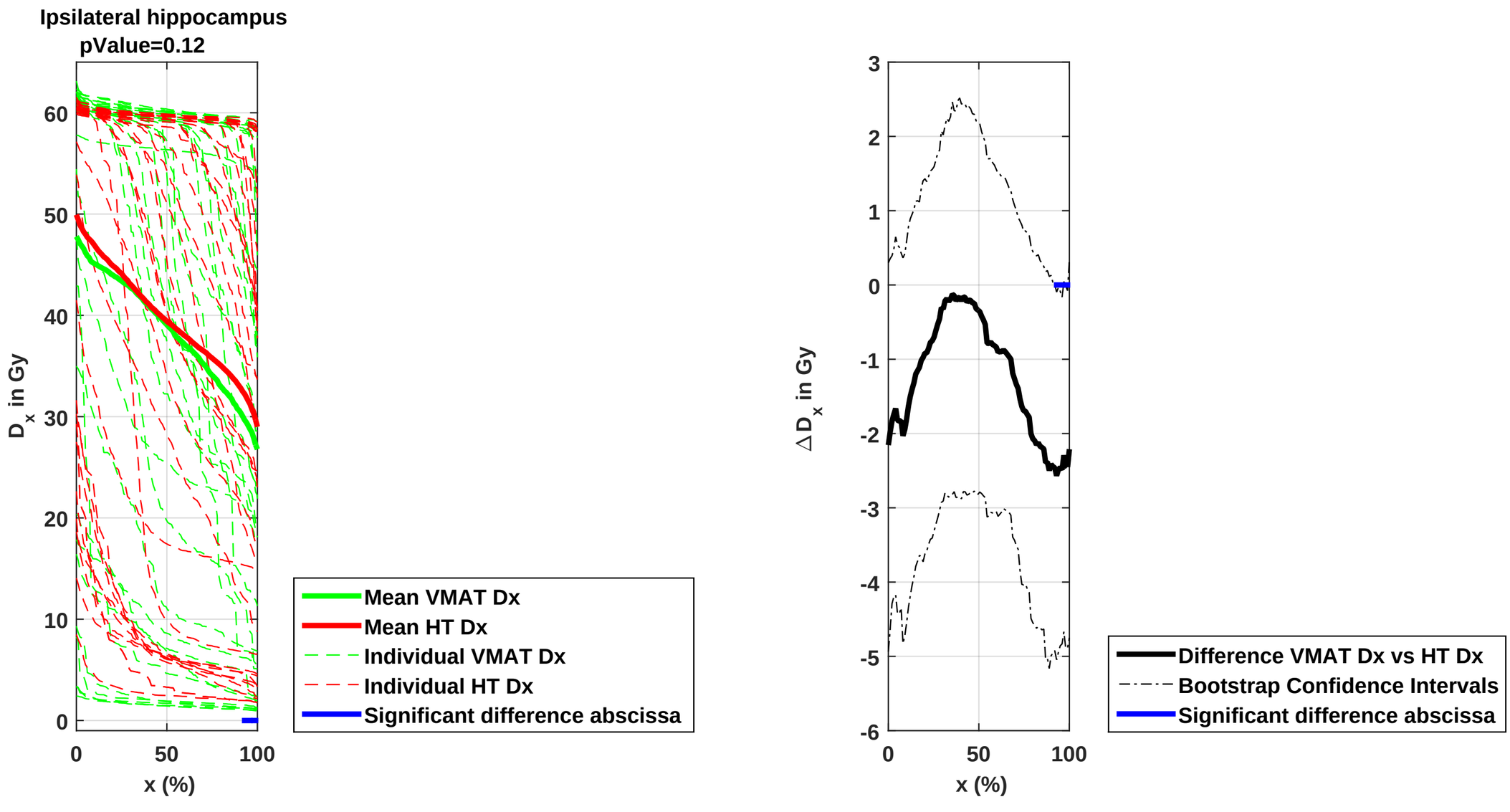
Ipsilateral hippocampus
pValue=0.12
D_x in Gy
x (%)
Mean VMAT Dx
Mean HT Dx
Individual VMAT Dx
Individual HT Dx
Significant difference abscissa
ΔD_x in Gy
x (%)
Difference VMAT Dx vs HT Dx
Bootstrap Confidence Intervals
Significant difference abscissa

Figure 4B

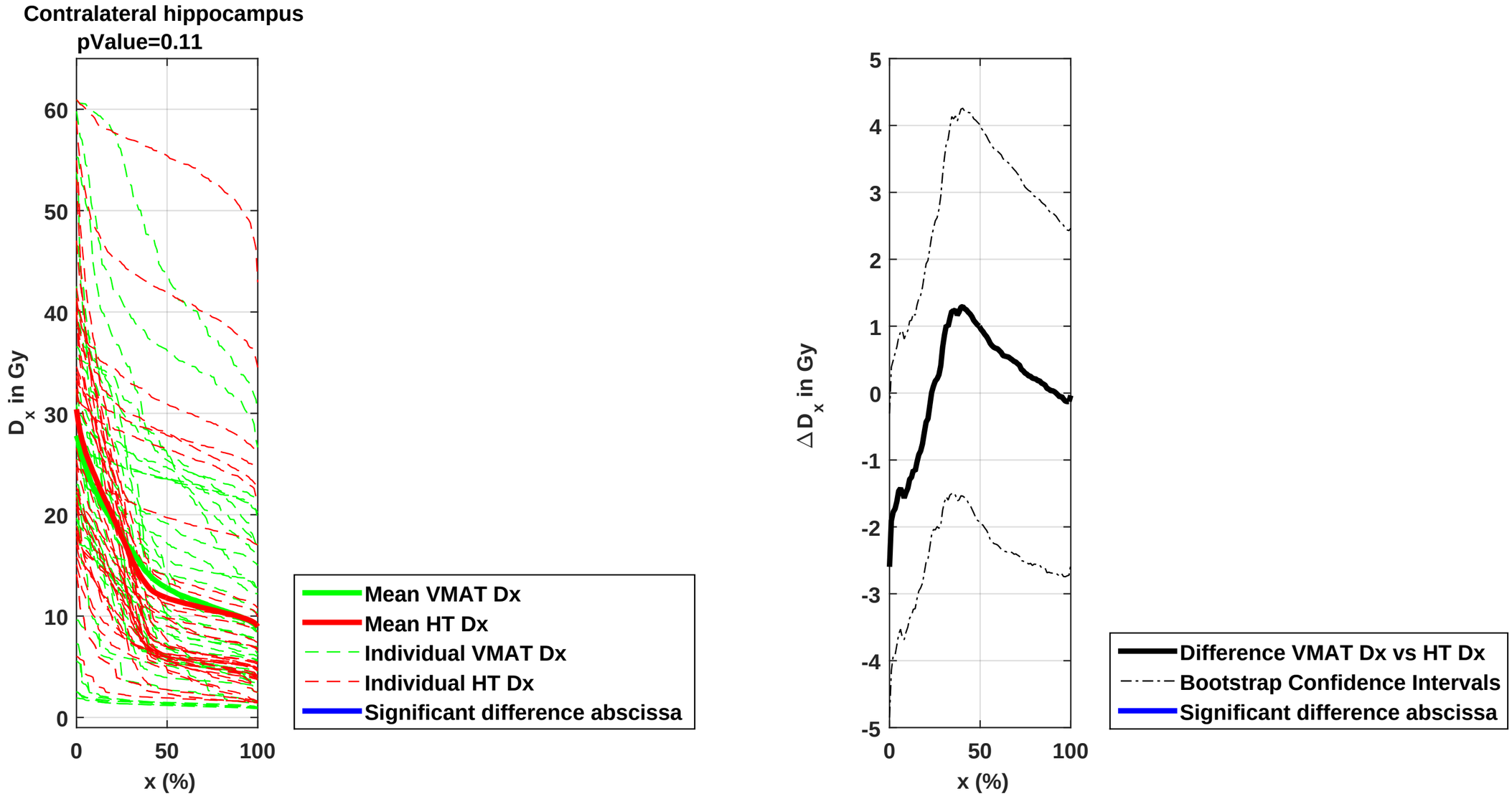
Contralateral hippocampus
pValue=0.11
D_x in Gy
x (%)
Mean VMAT Dx
Mean HT Dx
Individual VMAT Dx
Individual HT Dx
Significant difference abscissa
ΔD_x in Gy
x (%)
Difference VMAT Dx vs HT Dx
Bootstrap Confidence Intervals
Significant difference abscissa

Figure 5

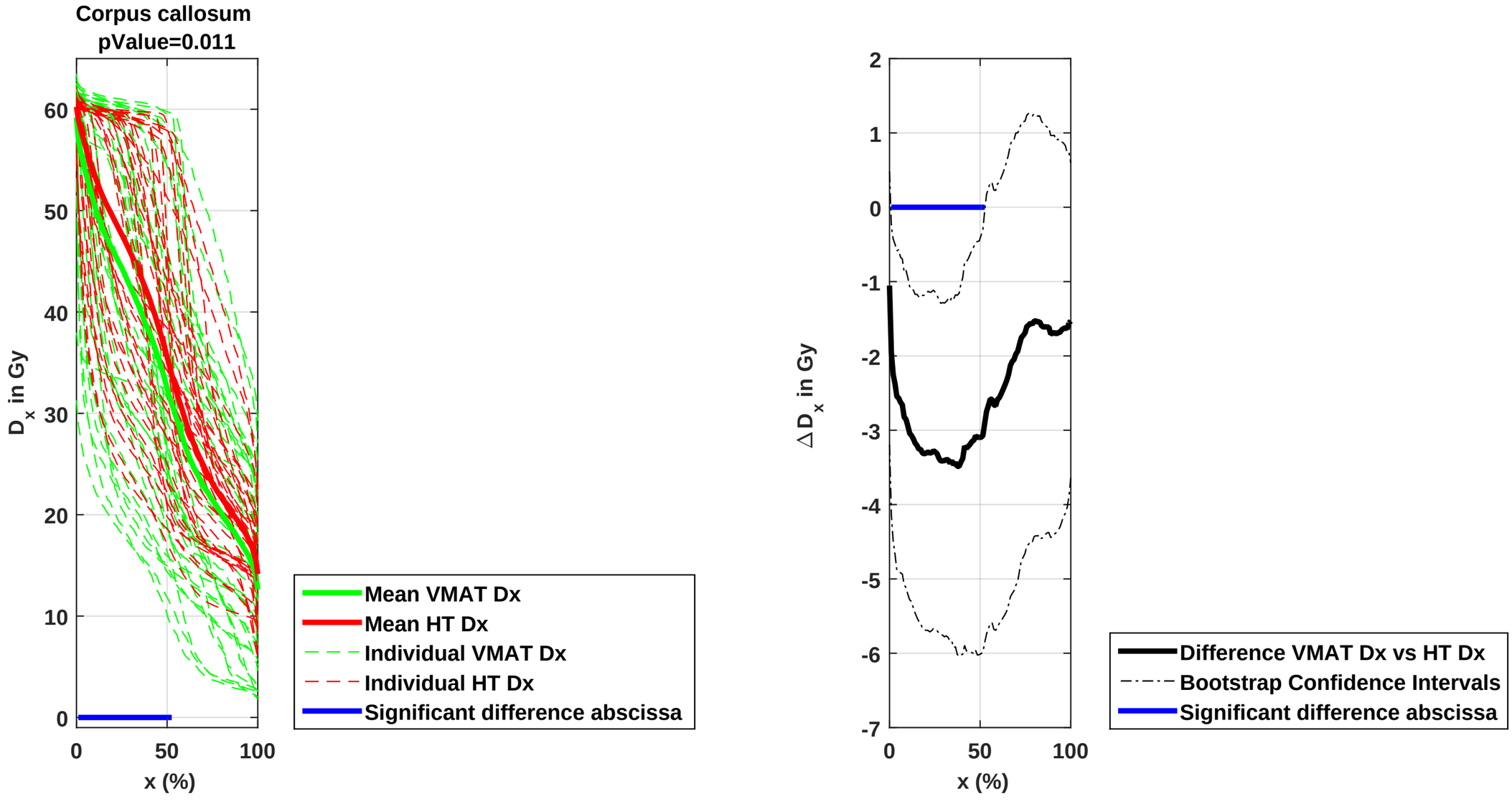
Corpus callosum
pValue=0.011
D_x in Gy
x (%)
Mean VMAT Dx
Mean HT Dx
Individual VMAT Dx
Individual HT Dx
Significant difference abscissa
ΔD_x in Gy
x (%)
Difference VMAT Dx vs HT Dx
Bootstrap Confidence Intervals
Significant difference abscissa

Figure 6A

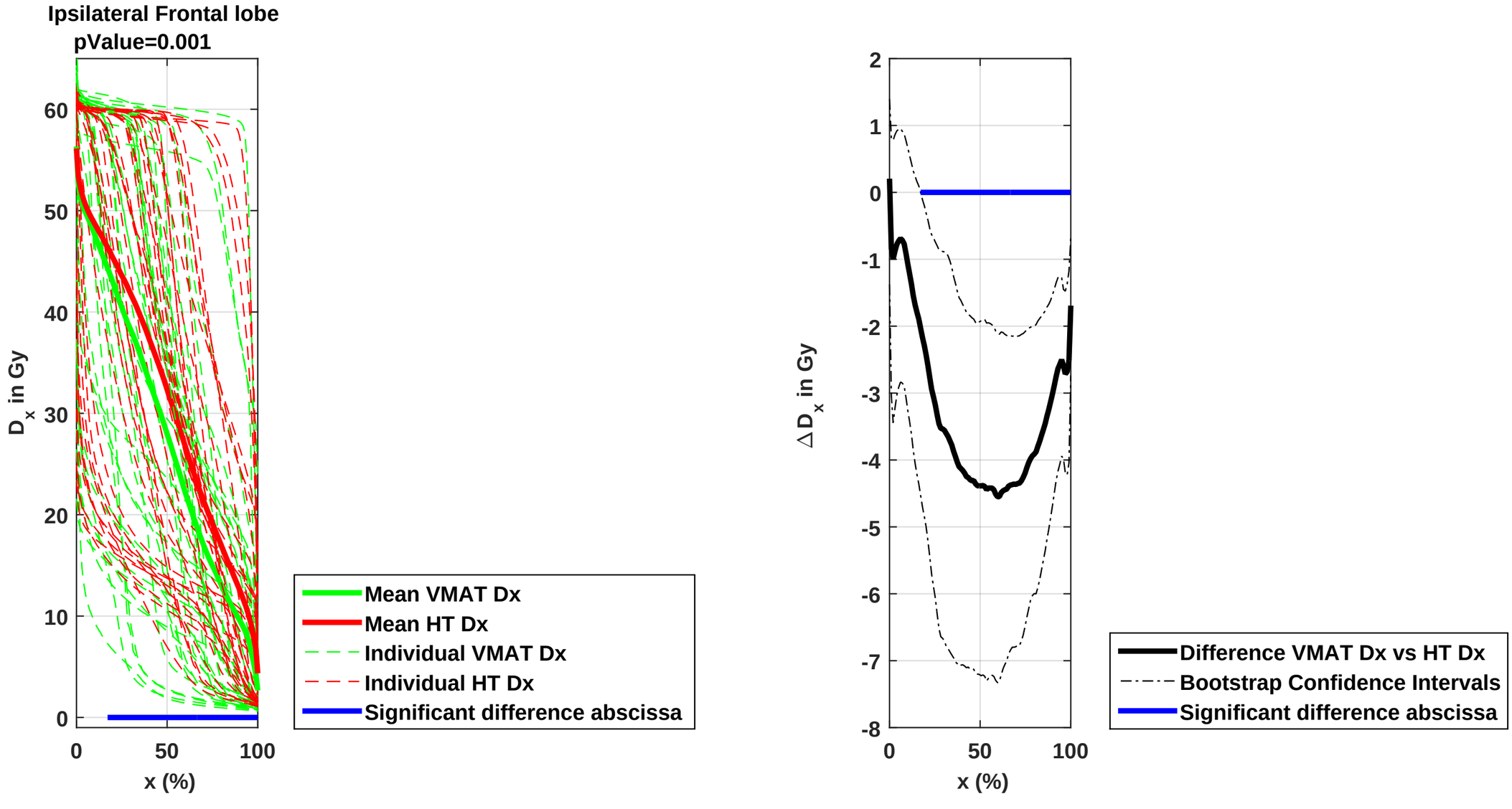
Ipsilateral Frontal lobe
pValue=0.001
D_x in Gy
x (%)
Mean VMAT Dx
Mean HT Dx
Individual VMAT Dx
Individual HT Dx
Significant difference abscissa
ΔD_x in Gy
x (%)
Difference VMAT Dx vs HT Dx
Bootstrap Confidence Intervals
Significant difference abscissa

Figure 6B

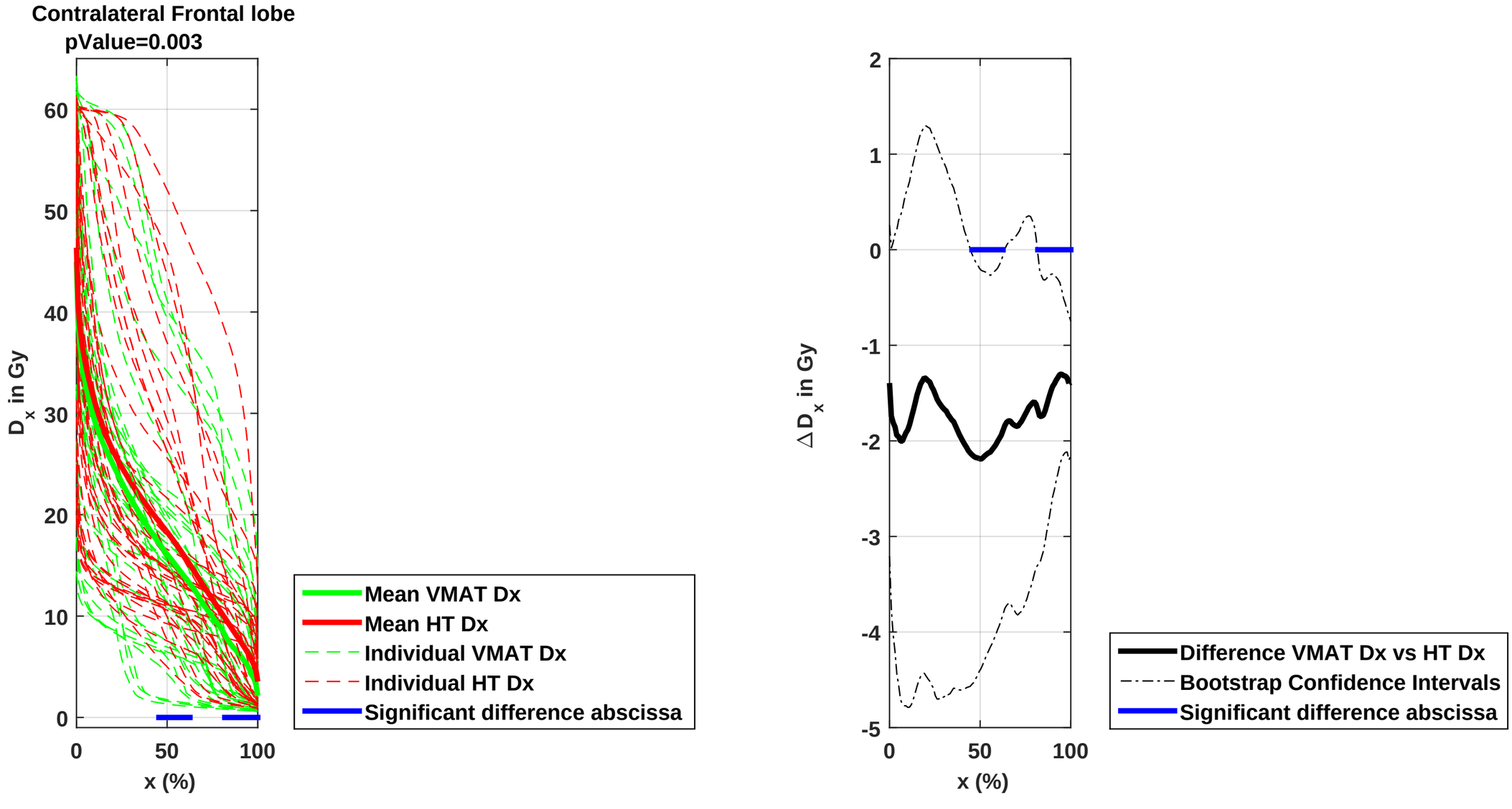
Contralateral Frontal lobe
pValue=0.003
D_x in Gy
x (%)
Mean VMAT Dx
Mean HT Dx
Individual VMAT Dx
Individual HT Dx
Significant difference abscissa
ΔD_x in Gy
x (%)
Difference VMAT Dx vs HT Dx
Bootstrap Confidence Intervals
Significant difference abscissa

Figure 7A

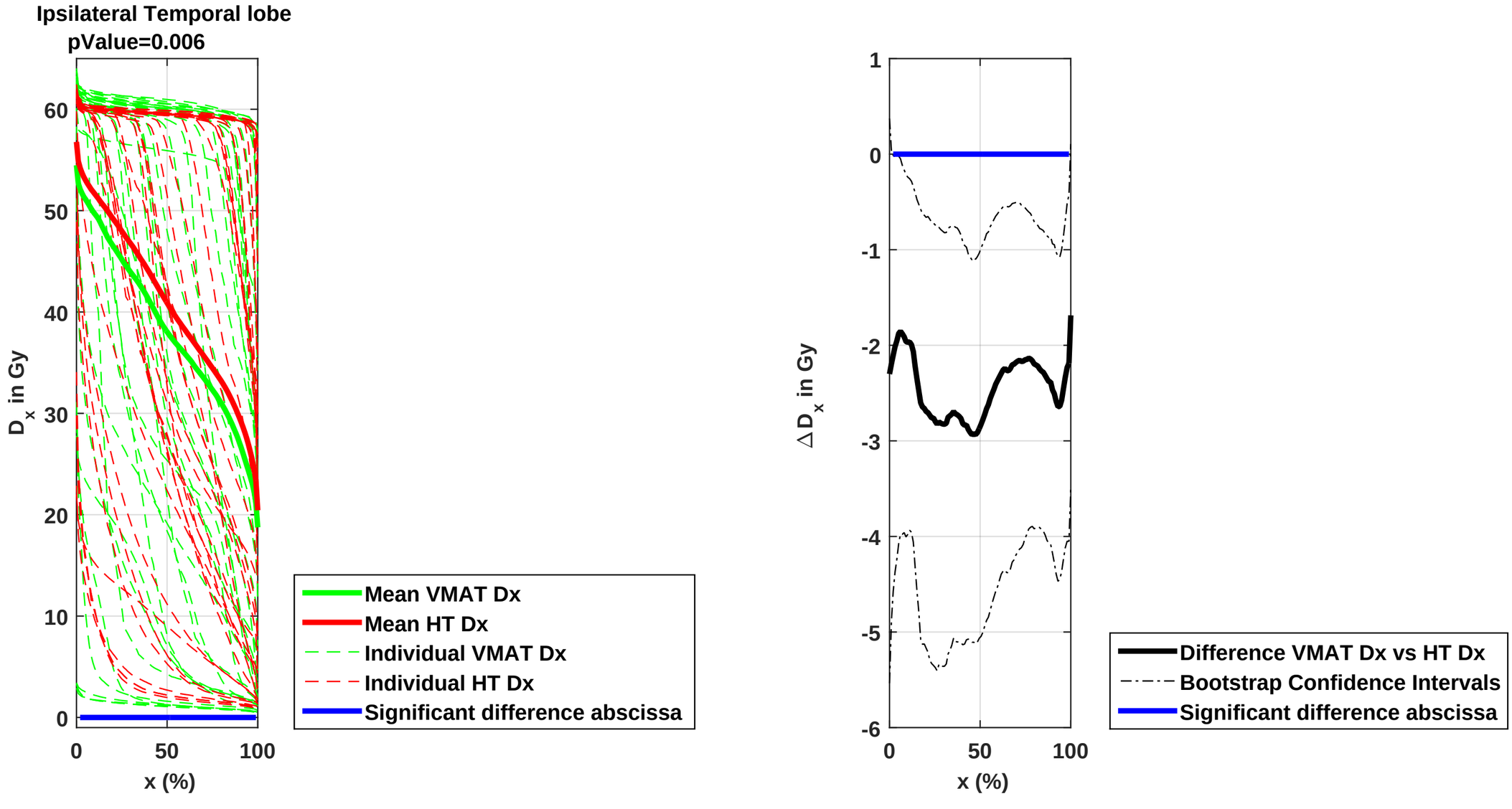
Ipsilateral Temporal lobe
pValue=0.006
D_x in Gy
x (%)
Mean VMAT Dx
Mean HT Dx
Individual VMAT Dx
Individual HT Dx
Significant difference abscissa
ΔD_x in Gy
x (%)
Difference VMAT Dx vs HT Dx
Bootstrap Confidence Intervals
Significant difference abscissa

Figure 7B

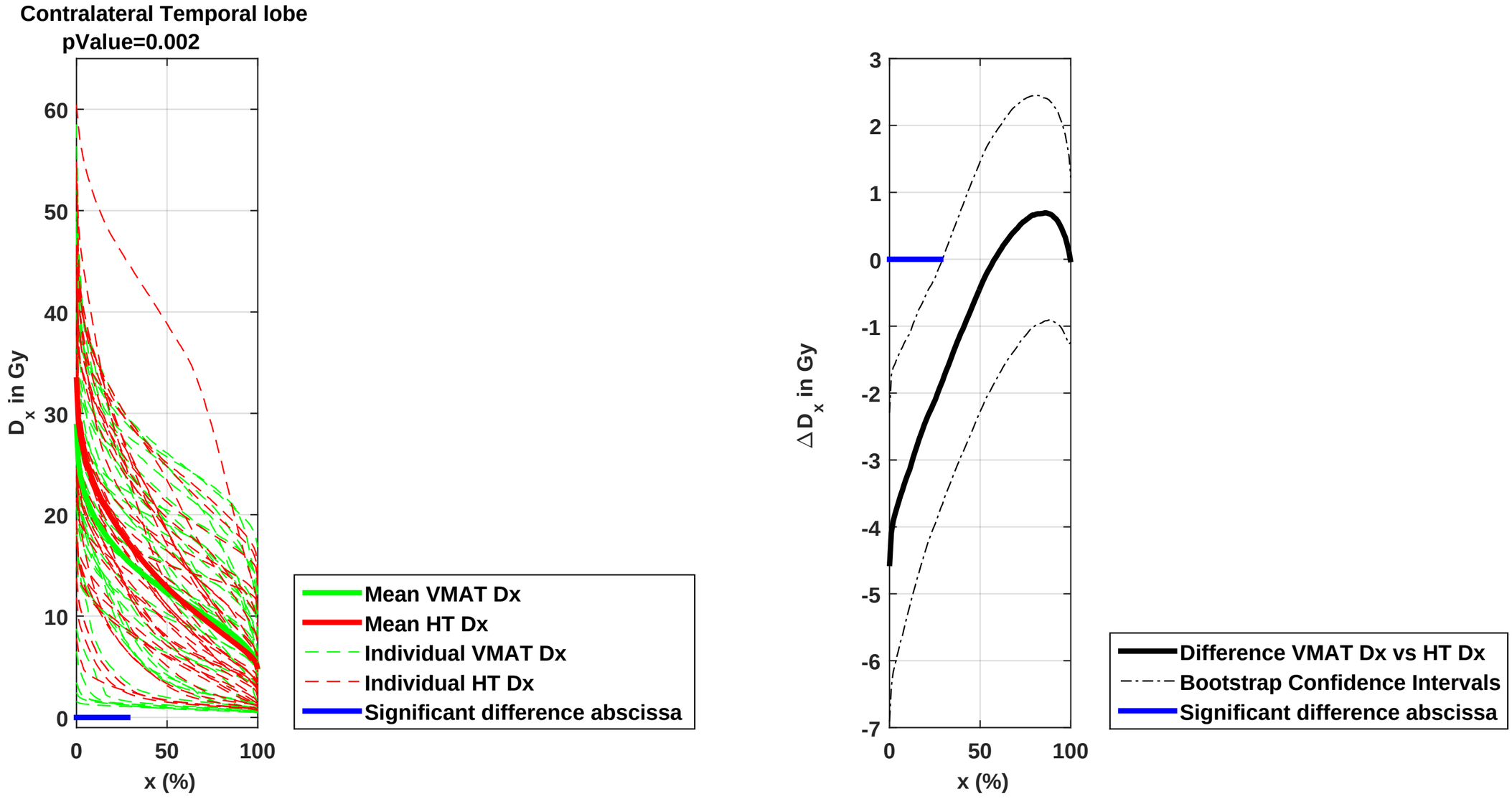
Contralateral Temporal lobe
pValue=0.002
D_x in Gy
x (%)
Mean VMAT Dx
Mean HT Dx
Individual VMAT Dx
Individual HT Dx
Significant difference abscissa
ΔD_x in Gy
x (%)
Difference VMAT Dx vs HT Dx
Bootstrap Confidence Intervals
Significant difference abscissa

Figure 8A

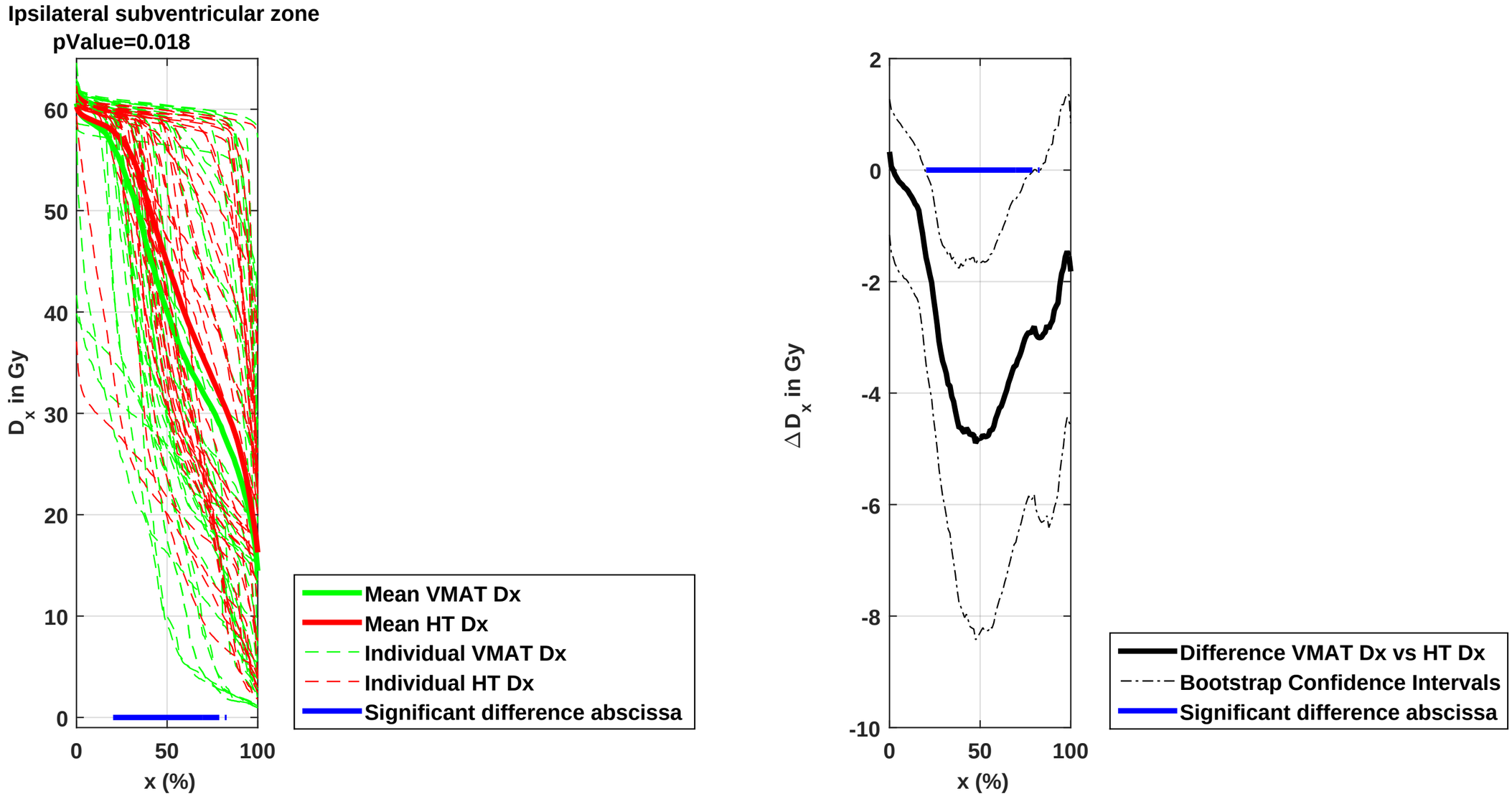
Ipsilateral subventricular zone
pValue=0.018
D_x in Gy
x (%)
Mean VMAT Dx
Mean HT Dx
Individual VMAT Dx
Individual HT Dx
Significant difference abscissa
ΔD_x in Gy
x (%)
Difference VMAT Dx vs HT Dx
Bootstrap Confidence Intervals
Significant difference abscissa

Figure 8B

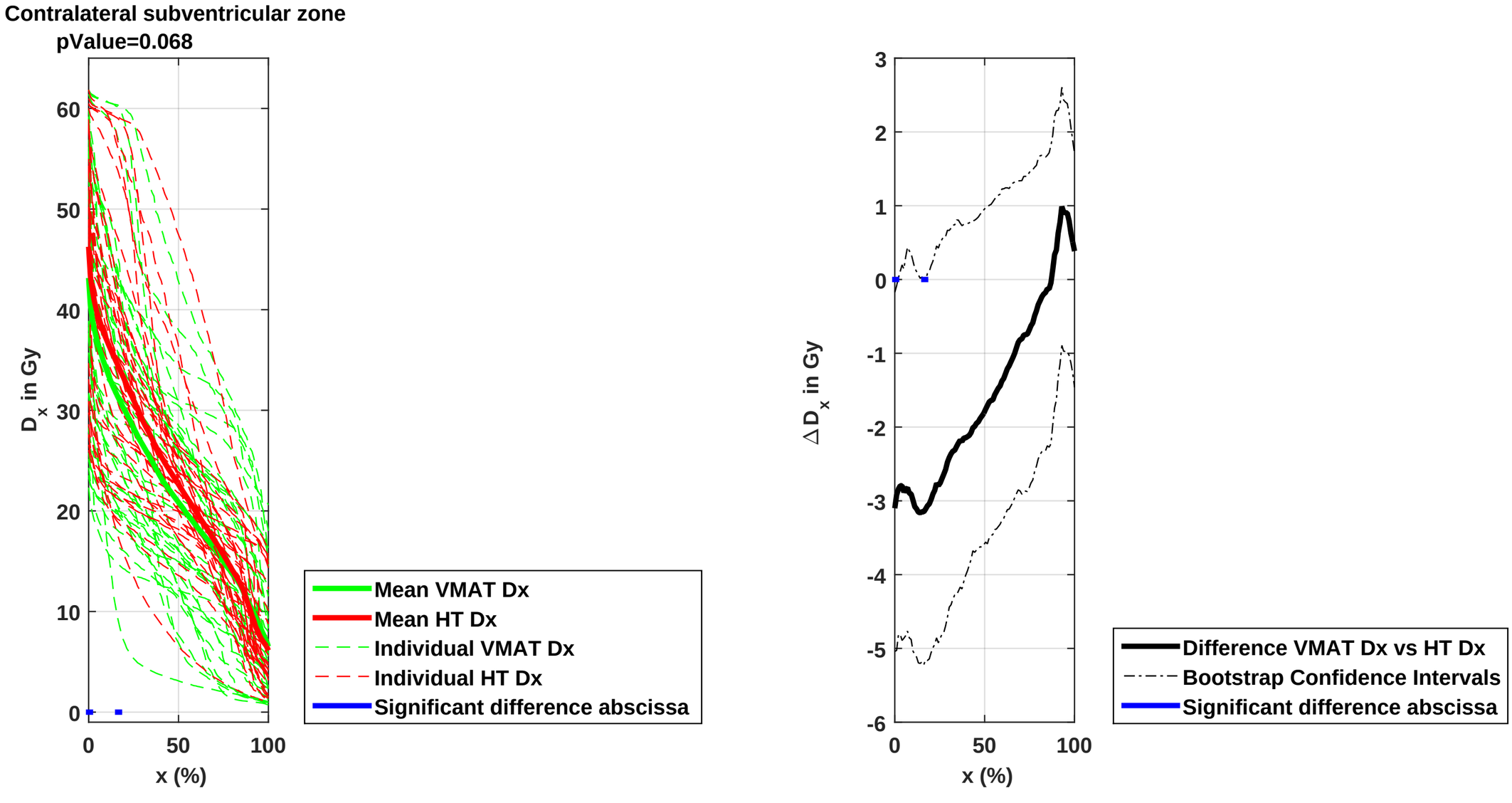
Contralateral subventricular zone
pValue=0.068
D_x in Gy
x (%)
Mean VMAT Dx
Mean HT Dx
Individual VMAT Dx
Individual HT Dx
Significant difference abscissa
ΔD_x in Gy
x (%)
Difference VMAT Dx vs HT Dx
Bootstrap Confidence Intervals
Significant difference abscissa